Distinction Between Hepatic Focal Nodular Hyperplasia and Malignant Liver Lesions Using Technetium-99m-Galactosyl-Neoglycoalbumin

Amir Kurtaran, Christian Müller, Gottfried Novacek, Klaus Kaserer, Mustafa Mentes, Markus Raderer, Johann Pidlich, Klemens Eibenberger, Peter Angelberger and Irene Virgolini

Departments of Nuclear Medicine, Gastroenterology, Pathology and Radiology, University of Vienna, Vienna; and Department of Radiochemistry, Research Center Seibersdorf, Seibersdorf, Austria

Distinction between hepatic focal nodular hyperplasia (FNH) and malignant liver lesions is essential because of the different therapy strategies, since FNH can be managed conservatively. The aim of this study was to describe the imaging pattern of FNH using the hepatocyte receptor ligand ^{99m}Tc-galactosyl-neoglycoalbumin (^{99m}Tc-NGA) and to assess the value of this receptor imaging agent in the differentiation of FNH from malignant liver lesions. **Methods:** Twelve consecutive patients with histologically confirmed FNH were investigated. The FNH-lesions were asymptomatic and incidentally found by ultrasonography. Nine patients with histologically verified hepatocellular carcinomas and three patients with liver metastases spread from gastrointestinal adenocarcinomas served as controls. **Results:** All FNH lesions showed normal or even increased uptake of ^{99m}Tc-NGA. Whereas malignant liver lesion-to-normal liver ratios amounted to 0.4 ± 0.2 (mean ± s.d.), FNH lesion-to-normal liver ratios were 1.7 ± 0.3 (mean ± s.d.). **Conclusion:** The receptor imaging agent ^{99m}Tc-NGA with concurrent use of SPECT is useful in the differential diagnosis of FNH and malignant hepatic tumors.

Key Words: hepatic focal nodular hyperplasia; technetium-99m-galactosyl-neoglycoalbumin; hepatocellular carcinoma

J Nucl Med 1997; 38:1912–1915

Focal nodular hyperplasia (FNH) is a benign hepatic tumor which characteristically occurs in women of reproductive age and is often discovered incidentally (*1,2*). A large number of imaging modalities have been used to evaluate FNH lesions, however, the differential diagnosis between FNH and malignant liver lesions continues to pose a diagnostic challenge (*2–4*). Ultrasonography (US), CT and MRI are sensitive, but cannot clearly differentiate benign lesions including FNH from primary hepatic malignancies (*2,5–10*). US can only be considered as a screening technique (*11*) and offers no tissue specificity (*5,7,12*), since FNH may appear hypoechoic, hyperechoic or even isoechoic (*11*). The CT characteristic of FNH is variably reported to be hyperdense or hypodense, and most lesions are hypervascular with intravenous contrast enhancement (*5,10*). CT lacks sensitivity (*7,10*) and it cannot reliably distinguish between FNH from HCC if the lesions are small-sized (*7*). MRI may give as an important pattern a central scar, however, the positive predictive value is low (*9,10*). The best imaging procedure in the diagnosis of FNH may be enhanced MRI with a sensitivity of 70% and a specificity of 98% (*11*). When the characteristic triad of isointensity on T1- and T2-weighted sequences, lesion homogenity and a central hyperintense scar on T2-weighted sequences is present, the diagnosis of FNH can be considered as certain.

Received Nov. 11, 1996; revision accepted Mar. 12, 1997.

For correspondence or reprints contact: Irene Virgolini, MD, Department of Nuclear Medicine, University of Vienna, Währinger Gürtel 18–20, Ebene 3L, A-1090 Vienna, Austria.

Scintigraphy might be useful in the diagnosis of FNH. The most helpful finding is evidence of normal or increased uptake on ^{99m}Tc-sulfur colloid in an area of FNH, which is based on the presence of Kupffer cells. However, ^{99m}Tc-sulfur colloid scintigraphy shows focal defects in about 30%–35% of patients with FNH (*10,13*) and the distinction between FNH and hepatic malignancies may not be possible (*11,14*). The hepatobiliary tracer trimethyl bromo-imino-diacetic acid (TBIDA) labeled with ^{99m}Tc may also be in some cases useful (*11*), however, liver metastases or HCC may exhibit a radioactivity uptake pattern similar to that of FNH, thus diminishing the specificity of this scintigraphy (*15*).

We have successfully used the hepatocyte-specific ligand ^{99m}Tc-galactosyl-neoglycoalbumin (^{99m}Tc-NGA) in combination with ^{123}I-Tyr-(A14)-insulin for the visualization of hepatocellular carcinomas (*16*). Technetium-99m-NGA is a ligand which maintains specific binding onto the hepatic binding protein receptor that resides exclusively at the cell surface membrane of liver cells (*17*). This study demonstrates ^{99m}Tc-NGA usefulness to distinguish FNH lesions from malignant liver lesions.

MATERIALS AND METHODS

Preparation and Labeling of NGA

Synthesis and preparation of NGA was done as described (*16,17*). A molar ratio of coupling agent/HSA of 138 was used, resulting in about 21 galactose residues per HSA molecule. NGA was labeled with ^{99m}Tc to yield a specific activity of 150 MBq/50 nmol NGA. The final ^{99m}Tc-NGA preparation was filtered through a sterile 0.2-μm membrane. Radiochemical purity was routinely monitored by cellulose-acetate electrophoresis in 0.1 *M* barbital buffer (pH 8.6) run at 300 V for 20 min and was >97%. The labeling yield after filtration amounted to about 95%; the in vitro stability at room temperature exceeded 24 hr.

Patients

Twelve patients (11 women, 1 man; age range 25–56 yr; mean age 34.6 ± 10.0 yr) with histologically confirmed FNH were enrolled in this study. FNH lesions were incidental ultrasonographic findings (Table 1). Additional imaging techniques included CT and/or MRI. The median size of the FNH lesions was 4 cm (range 2.5–7 cm). Histological examinations of the lesions were performed by unclear cases to exclude a malignancy. All the patients with histologically verified FNH had ^{99m}Tc-NGA scanning. Nine patients with histologically verified hepatocellular carcinomas (6 men, 3 women; age range 54–76 yr; mean age 58.5 ± 22.3 yr) and three patients (1 man, 2 women; age range 55–83 yr; mean age 65 ± 15.6 yr) with liver metastases spread from gastrointestinal adenocarcinomas served as controls.

TABLE 1
Technetium-99m-NGA Receptor Imaging of Histological Confirmed FNH

Patient no.	Sex	Age (yr)	CT/US/MRI finding-lesions localization size (cm)	Technetium-99m-NGA scintigraphy results
1	F	41	Segment VII/VIII 6 cm	Increased accumulation in lesion
2	F	26	Segment II 3 cm	Increased accumulation in lesion
3	F	50	Segment VI 3 cm	Normal accumulation in lesion
4	F	34	Segment VIII 2.5 cm	Normal accumulation in lesion
5	F	25	Segment VII 4 cm	Increased accumulation in lesion
6	F	43	Segment IV/VI 7 cm	Increased accumulation in lesion
7	F	56	Segment IV 3 cm	Normal accumulation in lesion
8	F	37	Segment II/III 6 cm	Increased accumulation in lesion
9	F	36	Segment VII 4 cm	Normal accumulation in lesion
10	F	28	Segment II/III 7 cm	Increased accumulation in lesion
11	F	30	Segment VI 3 cm	Increased accumulation in lesion
12	F	26	Segment VI/VIII 5 cm	Increased accumulation in lesion

Gamma Camera Imaging

The patients were positioned under a gamma camera equipped with a low energy ultrahigh resolution parallel collimator (LEUHR-PAR) (Picker Prism 1000, Bedford Hts., OH). Ten minutes after injection of 120–160 MBq ^{99m}Tc-NGA, static planar imaging of the liver in anterior, posterior and right lateral projection were performed, and 800 Kcts were acquired for each view. In all patients, SPECT acquisitions (128 × 128 matrix, 360° (6°/step), three-headed Picker 3000-gamma camera, LEUHR-PAR collimator, ramp filtered backprojection, three-dimensional low-pass postfiltering) were performed. Late static imaging of the liver was also done 2–3 hr after injection. The interpretation of the scans was performed by two nuclear medicine physicians.

Quantification Methods

We used a manually drawn region of interest (ROI) of the lesions visualized on to ^{99m}Tc-NGA (seen also on CT and/or MRI). The ROIs were drawn by two independent observers and the average (counts/pixels) was accepted as ROI number 1. A second ROI was placed over the whole liver and accepted as ROI 2. ROI 2 served as background. Counts/pixels were calculated using the Picker Prism 1000 computer system for ROI 1 as well as for ROI 2. The calculated values of counts/pixels for all malignant liver lesions were compared to counts/pixels of FNH lesions.

RESULTS

All patients had a solitary FNH lesion. In 8 of 12 patients, the FNH lesion was visualized as a hot spot (66%) (Table 1). In the remaining four patients (34%), the accumulation of ^{99m}Tc-NGA was indistinguishable from the surrounding normal liver tissue. All malignant liver lesions showed a significantly decreased accumulation of ^{99m}Tc-NGA (cold spots). Whereas malignant liver lesion-to-normal liver ratios amounted to 0.4 ± 0.2 (mean ± s.d.), FNH lesion-to-normal liver revealed a ratio of 1.7 ± 0.3 (mean ± s.d.).

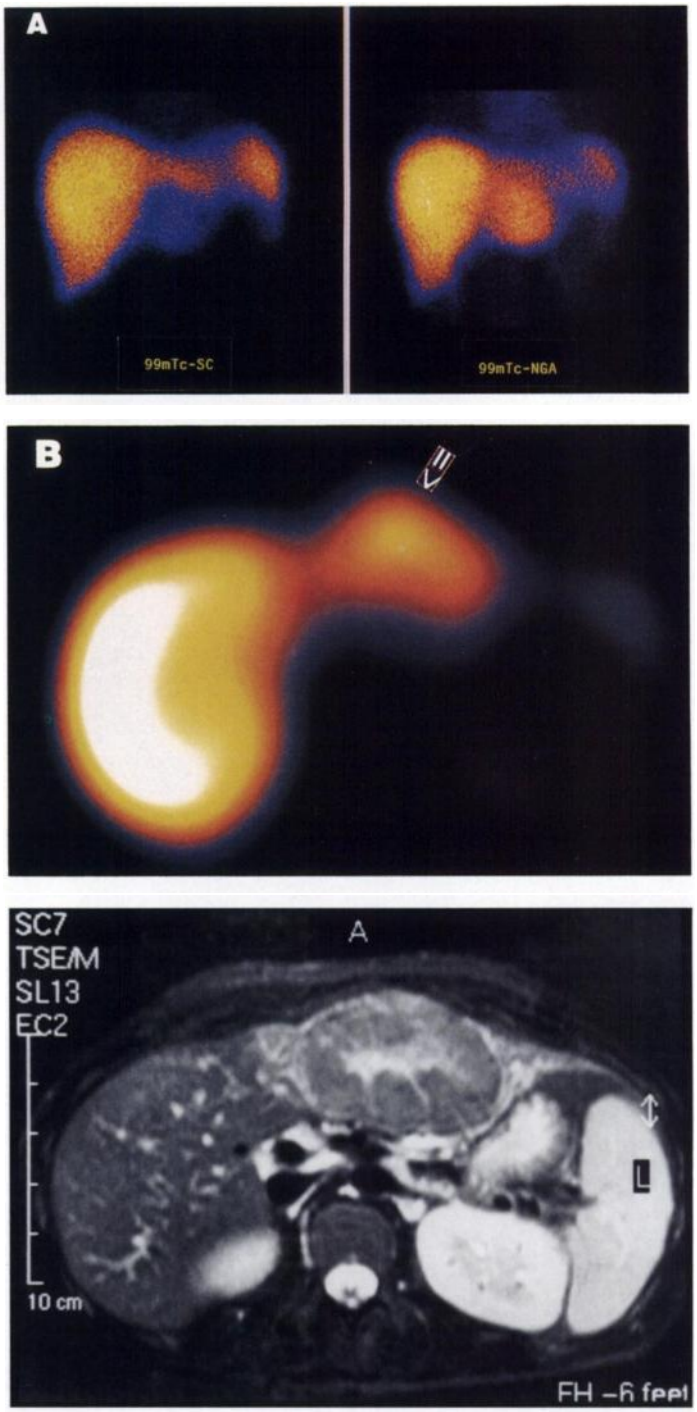

FIGURE 1. Technetium-99m-SC and ^{99m}Tc-NGA scintigraphy in Patient 10. (A) The sulfur chloride scintigraphy (anterior planar scintigraphy) demonstrates a cold spot in the left liver lobe (left), whereas the ^{99m}Tc-NGA scintigraphy (right) shows a significantly increased uptake in this lesion (arrow). (B) SPECT study (transverse slice) of the same patient (arrow). (C) Corresponding MRI.

DISCUSSION

FNH is a benign hepatic tumor which characteristically occurs in women of reproductive age (*1*). In about 80% of cases, the lesion is discovered incidentally (*2*), however, occasionally abdominal pain can be present in these patients (*5*). The pathogenesis of FNH is not well understood, the often reported association with use of contraceptives is probably incidental (*2*). Proposed mechanisms include compensatory regeneration from localized injury related to vascular anomaly, hepatocellular proliferation induced by vascular injury (*2*) or a reaction to a localized vascular anomaly (*3*).

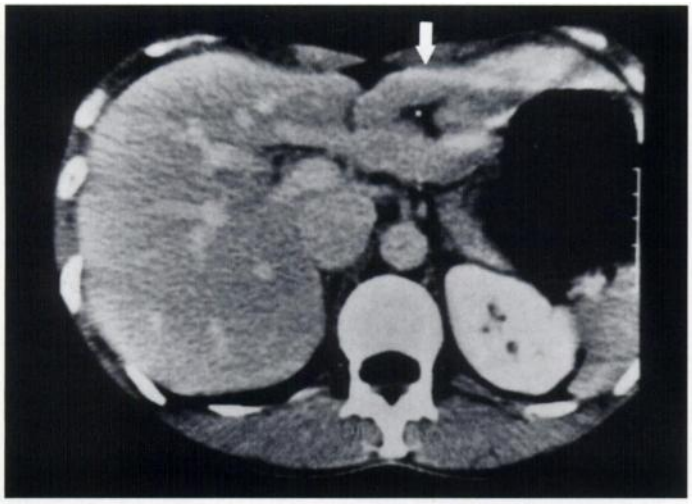

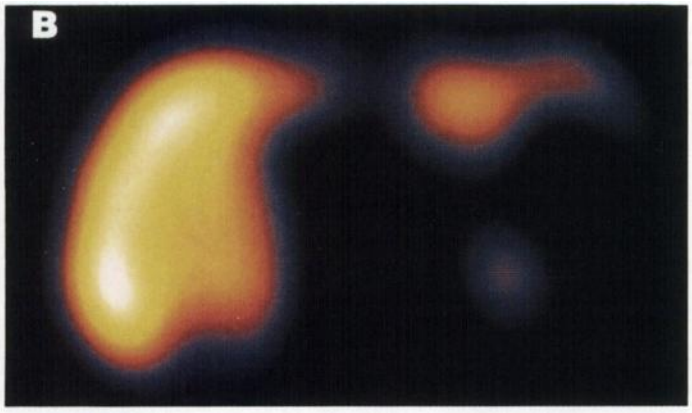

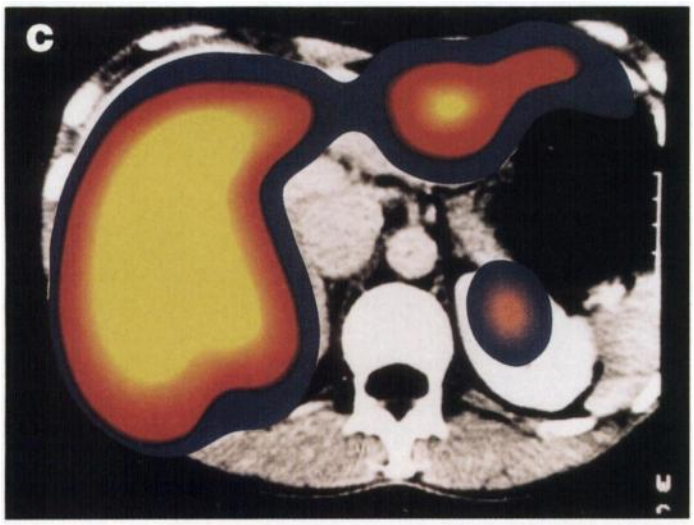

FIGURE 2. Technetium-99m-NGA scintigraphy in Patient 8. (A) CT study of a lesion (arrow) in segment II/III. The accumulation of ^{99m}Tc-NGA in the liver is significantly increased in segment II/III (B) indicating the FNH lesion. (C) SPECT image superimposed on the CT for a precise localization.

In this study, we report that FNH shows normal or even increased accumulation of ^{99m}Tc-NGA (Table 1), while malignant liver lesions appear as cold spots on ^{99m}Tc-NGA scans (*16*). Technetium-99m-NGA scintigraphy of the liver is based on visualization of the receptor binding of ^{99m}Tc-NGA to liver cells. In general, the accumulation of ^{99m}Tc-NGA is related to the functional activity and to the number of the functioning hepatocytes. A localized area of decreased accumulation of ^{99m}Tc-NGA can be expected where a decreased number of NGA-receptors is present. It is well known that the receptor-mediated binding and subsequent cellular endocytosis does not occur in HCC or metastatic tumors because surface NGA-receptors are lost during malignant de-differentiation (*16–24*). This imaging technique is similar to ^{99m}Tc-sulfur colloid, where normal or increased uptake on ^{99m}Tc-sulfur colloid is helpful in the diagnosis of FNH. However, ^{99m}Tc-sulfur colloid scintigraphy shows focal defects in about 30%–35% of patients with FNH (*10,13*) and the distinction between FNH and hepatic malignancies may not be possible (*11,14*). It was suggested that the biliary tracer, TBIDA, might be useful (*11*), however, liver metastases or HCC may show a radioactivity uptake pattern similar to that of FNH, diminishing the specificity of this scan (*15*). In cases of FNH, the function of the hepatocytes is normal and the surface receptors of NGA are probably intact. This finding could be the reason for the finding of normal or even increased accumulation, since the uptake of ^{99m}Tc-NGA depends on the presence of normally functioning hepatocytes. Therefore, only lesions that consist of functioning liver tissue can evoke the phenomenon of a "hot spot" or "normal uptake" on the ^{99m}Tc-NGA liver scanning.

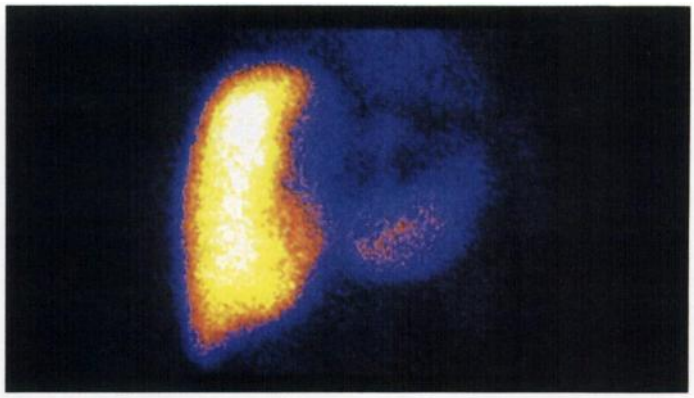

FIGURE 3. Technetium-99m-NGA scan of a patient with HCC showing a significant cold spot in the left liver lobe.

The main finding of our study is the demonstration that FNH shows normal or increased uptake based on receptor binding which enables the differentiation of FNH from malignant liver lesions. Recently, two hepatocyte-specific tracers, ^{99m}Tc-NGA and ^{123}I-Tyr-(A14)-insulin were used in patients with malignant hepatic tumors (*16*): if a lesion detected on US/CT or MRI shows a normal or increased accumulation of ^{99m}Tc-NGA, a benign lesion is present. For the differentiation of FNH from other hepatic lesions such as benign hepatic adenoma and hemangioma further studies are needed. In the case of a cold spot, a ^{123}I-Tyr-(A14)-insulin scintigraphy is indicated. Accumulation of ^{123}I-Tyr-(A14)-insulin in the lesion indicates a HCC lesion, whereas a matched defect can be considered to present a liver metastasis.

CONCLUSION

The hepatocyte-specific ligand ^{99m}Tc-NGA is clinically useful to differentiate FNH from malignant liver lesions. This method can provide a quick and safe identification of liver lesions seen on US, CT or MRI.

ACKNOWLEDGMENTS

We thank the nursing staff of the Department of Gastroenterology (Sr. Trude and team) for their excellent cooperation. This study was supported by the Austrian National Bank, Jubiläumsfonds, Austria.

REFERENCES

1. Edmondson HA, Peters RL. Tumors of the liver: pathologic features. *Semin Roentgenol* 1983;18:75–83.

2. Rogers JV, Mack LA, Freeny PC, et al. Hepatic focal nodular hyperplasia: angiography, CT, sonography, and scintigraphy. *Am J Roentgenol* 1981;137:983–990.
3. Yoshikawa J, Matsui O, Kadoya M, et al. Delayed enhancement of fibrotic areas in hepatic masses: CT-pathologic correlation. *J Comp Assist Tomogr* 1992;16:206–211.
4. Lee MJ, Saini S, Hamm B, et al. Focal nodular hyperplasia of the liver: MR findings in 35 proved cases. *Am J Roentgenol* 1991;156:317–320.
5. Shirkhoda A, Farah MC, Bernacki, et al. Hepatic focal nodular hyperplasia: CT and sonographic spectrum. *Abdom Imaging* 1994;19:34–38.
6. Kudo M, Tomita S, Tochio H, et al. Hepatic focal nodular hyperplasia: specific findings at dynamic contrast-enhanced US with carbon dioxide microbubbles. *Radiology* 1991;179:377–382.
7. Mathieu D, Bruneton JN, Drouillard J, et al. Hepatic adenoma and focal nodular hyperplasia: dynamic CT study. *Radiology* 1986;160:53–58.
8. Mattison GR, Glazer GM, Quint LE, et al. MR imaging of hepatic focal nodular hyperplasia: characterization and distinction from primary hepatic tumors. *Am J Roentgenol* 1987;148:711–715.
9. Butch RJ, Stark DD, Malt RA. MR imaging of hepatic focal nodular hyperplasia. *J Compt Assist Tomogr* 1986;10:874–877.
10. Nagorney DM. Benign hepatic tumors: focal nodular hyperplasia and hepatocellular adenoma. *World J Surg* 1995;19:13–18.
11. Cherqui D, Rahmouni A, Charlotte F, et al. Management of focal nodular hyperplasia and hepatocellular adenoma in young women: a series of 41 patients with clinical, radiological, and pathological correlations. *Hepatology* 1995;22:1674–1681.
12. Sandler MA, Petrocelli RD, Marks DS, et al. Ultrasonic features and radionuclide correlation in liver cell adenoma and focal nodular hyperplasia. *Radiology* 1980;135: 393–397.
13. Biersack HJ, Thelen M, Torres JF, et al. Focal nodular hyperplasia of the liver as established by ^{99m}Tc-sulfur colloid and HIDA scintigraphy. *Radiology* 1980;137:187–190.
14. Shortell CK, Schwartz SI. Hepatic adenoma and focal nodular hyperplasia. *Surg Gynecol Obstet* 1991;173:426–431.
15. Calvet X, Pons F, Bruix J, et al. Technetium-99m-DISIDA hepatobiliary agent in diagnosis of hepatocellular carcinoma: relationship between detectability and tumor differentiation. *J Nucl Med* 1988;29:1916–1920.
16. Kurtaran A, Li SR, Raderer M, et al. Technetium-99m-galactasyl-neoglycoalbumin combined with iodine-123-(A14)-insulin visualizes human hepatocellular carcinomas. *J Nucl Med* 1995;36:1875–1881.
17. Virgolini I, Müller C, Klepetko W, et al. Decreased hepatic function in patients with hepatoma or liver metastasis monitored by hepatocytes specific galactosylated radioligand. *Br J Cancer* 1990;61:937–941.
18. Kudo M, Vera DV, Stadalnik RC. Hepatic receptor imaging using radiolabeled asialoglycoprotein analogs. In: Lee YC, Lee RT, eds. *Neoglycoconjugates: preparation and applications*. Orlando: Academic Press 1994;11:373–402.
19. Hickman J, Ashwell G. Studies on the hepatic binding of asiologlycoproteins by hepatoma tissue and by isolated hepatocytes. In: Tager JM, Hooghwinkel GJM, Daems WT, eds. *Enzyme therapy in lysosomal storage disease*. North-Holland, Amsterdam; 1974:169–172.
20. Stockert RJ, Becker FF. Diminished hepatic binding protein for desialy glycoproteins during chemical hepatocarcinogenesis. *Cancer Res* 1980;40:3632–3634.
21. Sawamura T, Nakada H, Hazama H, et al. Hyperasiologlyco-proteinemia in patients with chronic liver diseases and/or liver cell carcinomas. Asiologlycoprotein receptor in cirrhosis and liver cell carcinoma. *Gastroenterology* 1984;87:1217–1221.
22. Reimer P, Weissleder R, Lee AS, et al. Receptor imaging: application to MR imaging of the liver cancer. *Radiology* 1990;177:729–734.
23. Virgolini I, Kornek G, Höbart J, et al. Scintigraphic evaluation of functional hepatic mass in patients with advanced breast cancer. *Br J Cancer* 1993;68:549–554.
24. Virgolini I, Muller C, Hobart J, et al. Liver function in acute viral hepatitis as determined by a hepatocyte-specific ligand: ^{99m}Tc-galactosyl-neoglycoalbumin. *Hepatology* 1992;15:593–598.

Technetium-99m-Furifosmin as an Agent for Functional Imaging of Multidrug Resistance in Tumors

James R. Ballinger, Tassawwar Muzzammil and Malcolm J. Moore

Faculties of Pharmacy and Medicine, University of Toronto; Departments of Oncologic Imaging and Medical Oncology, Princess Margaret Hospital; and Division of Experimental Therapeutics, Ontario Cancer Institute, Toronto, Ontario, Canada

There has been a preliminary report that furifosmin, like the other lipophilic ^{99m}Tc cations sestamibi and tetrofosmin, is a substrate for P-glycoprotein, the membrane transporter that is a mechanism of multidrug resistance (MDR) in tumors. This has been further investigated in the rat mammary carcinoma cell line MatB/WT and its doxorubicin-selected resistant variant MatB/AdrR. **Methods:** In vitro studies were performed by adding furifosmin to stirred single-cell suspensions of MatB/WT and MatB/AdrR in the presence or absence of the Pgp-modulating drug PSC833. Dynamic imaging studies over 30 min were performed in rats bearing MatB/WT or MatB/AdrR tumors growing in the leg. **Results:** Accumulation of furifosmin in MatB/AdrR cells in vitro was much lower than that in MatB/WT cells. The addition of 1 μM PSC833 increased the plateau accumulation in MatB/AdrR cells 2.4-fold, but did not affect accumulation in MatB/WT cells. In rats, furifosmin accumulated rapidly in MatB/WT tumors and washed out with a mean t_3 of 78 min. Washout from MAtB/AdrR tumors was more rapid, with a t_3 of 46 min ($p < 0.025$). Following dissection of animals at 30 min, mean tumor-to-muscle ratios were 1.57 and 1.05 in MatB/WT and MatB/AdrR tumors, respectively ($p < 0.025$). **Conclusion:** Furifosmin is suitable for functional imaging of multidrug resistance in tumors.

Key Words: technetium-99m-furifosmin; multidrug resistance; P-glycoprotein; breast cancer

J Nucl Med 1997; 38:1915–1919

Received Dec. 12, 1996; revision accepted Feb. 28, 1997.
For correspondence or reprints contact: J.R. Ballinger, PhD, Ontario Cancer Institute, 610 University Ave., Toronto, Ontario, Canada, M5G 2M9.

Though developed as agents for myocardial perfusion imaging, both sestamibi and tetrofosmin have been useful for tumor imaging (*1–6*). In particular, sestamibi has been evaluated extensively for scintimammography and may play a role when the mammogram is indeterminate and in women who have dense breasts or who have had previous breast surgery (*7–9*). In screening the accumulation of sestamibi in a variety of tumor cell lines in vitro, Piwnica-Worms' group noted that certain cell lines accumulated very little sestamibi (*10*). They later correlated this low accumulation with overexpression of P-glycoprotein (Pgp), a transmembrane pump that is a mechanism of multidrug resistance (MDR) in tumors (*11*). This work has been extended to insect cells transfected with the human *MDR1* gene (*12*) and to an animal model (*13*). Del Vecchio's group from Naples has presented results which show a correlation between sestamibi efflux rates and Pgp expression in biopsy samples (*14,15*) and response to chemotherapy (*16*) in patients with breast cancer. Other authors have also suggested that low accumulation of sestamibi corresponds to MDR in patients with lymphoma (*17*) and lung cancer (*18*).

We have demonstrated that tetrofosmin, a myocardial perfusion agent that is a phosphine rather than an isonitrile, is also a substrate for Pgp in vitro and has properties very similar to sestamibi (*19*).

Furifosmin is another ^{99m}Tc-labeled myocardial perfusion agent (*20*) that has been shown to be a substrate for Pgp in vitro (*21*). We have further evaluated this phenomenon, extending studies to an in vivo model of breast cancer, the results of which